Structural and electronic properties of Fe and TiFe from extended and near-edge x-ray-absorption structure

N. Motta

Scuola Normale Superiore, Pisa, Italy

M. De Crescenzi

*Dipartimento di Fisica, Università degli Studi di Calabria,
Arcavacata di Rende, I-87100 Cosenza, Italy*

A. Balzarotti

Istituto di Fisica, Università degli Studi di Roma II, I-00173 Roma, Italy

The extended x-ray-absorption fine structure of Fe and TiFe has been measured above the K edges of Fe and Ti at 80 and 300 K. In both materials the fifth and sixth coordination shells show clear evidence of multiple-scattering effects due to the intervening first- and second-shell atoms. The plane-wave approximation for the scattering is found to be inadequate and corrections for the wave curvature are made to the backscattering phase shifts of the first shell. The first peak of the radial distribution function of Fe and TiFe is decomposed into its constituents by means of the beat method. The local order of TiFe around both Ti and Fe atoms is good up to the sixth coordination shell. It is shown that the near-edge structure of both Ti and Fe K edges of TiFe reflects the local state density of p-like symmetry at the titanium site, in agreement with detailed partial—density-of-states calculations.

I. INTRODUCTION

The transition-metal alloys of the Asano type are characterized by a relatively narrow range of atomic composition in comparison with the solid-solution alloy phase. They have a simple and stable ordered lattice of cesium chloride (CsCl) structure and a tendency to form binary compounds with an approximately symmetrical disposition around the chromium group. In particular, titanium-group elements tend to combine with iron-group elements, while scandium-group elements choose partners from the copper and zinc groups. TiFe is one of these alloys which exhibits a very stable lattice and it is a material of technological interest because of its ability to incorporate large quantities of atomic hydrogen at modest pressures.[1] Several investigations aiming to clarify how the interstitial hydrogen interacts with the lattice have been recently undertaken. In such a context, knowledge of the local order and of the electronic properties of the crystal could be of relevance as a basis to understand their possible modifications in the presence of large amounts of atomic hydrogen.

X-ray analysis in combination with thermal methods has been used to determine the composition and the stability of the titanium-iron alloys at different temperatures. For TiFe the lattice parameter is 2.978 Å (Refs. 2 and 3) and no CsCl-type superlattice lines have been observed. However, this may be a result of too small a difference between the atomic scattering power of the components and it does not prove the absence of ordering. Nevertheless, substitutional disorder might be present locally due to the narrow range of the phase diagram in which the 50%-50% composition is stable.

The electronic structure of TiFe has been theoretically studied by Yamashita and Asano[4] and by Papaconstantopoulos[5,6] who have calculated partial and total densities of the valence and conduction bands. They found that the valence band is mainly Fe-like and the conduction band is mainly Ti-like with a minimum density in the middle region. The Fermi energy lies slightly above the minimum of the density of states. A deep valley in the density of states is characteristic of the ordered alloy, while in the disordered phase this gap tends to be filled up. In TiFe the theoretical partial density of states of Ti shifts upward relative to that of Fe and changes significantly if lattice disorder is present and the high stability of the ordered lattice is lost.

The present investigation was undertaken to test the local ordering around each atomic constituent of the alloy by relying on the potential of the extended x-ray-absorption fine-structure (EXAFS) and x-ray-absorption near-edge structure (XANES) techniques.

As is well known, EXAFS is sensitive to pairwise atomic correlations, as implied by the single-scattering approximation, while XANES yields higher-order correlations, i.e., bond angles and distances, and then is related directly to the electronic structure.

By modeling the radial distribution function of Fe with the known scattering and lattice parameters, we conclude that the local order of TiFe up to the sixth coordination shell is as good as in Fe, both around Ti and Fe. For comparison purposes we have studied the EXAFS spectrum of the crystalline Fe which has a lattice parameter close to that of TiFe, and which has the same bcc lattice. Evidence is found in both materials of large focusing effects for the outer shells, due to multiple-scattering processes involving linear scattering paths. The backscattering phases for the first two shells have been corrected to include the curvature of the outgoing photoelectron wave.

The analysis of XANES in terms of projected density of states at both Fe and Ti sites strongly supports an ordered environment of CsCl type, as theoretically discussed by Yamashita and Asano.[4] A clear indication is found of the titanium character of the p-like densities of the conduction states of TiFe at the Ti and Fe K edges, in full agreement with theoretical predictions.

In Sec. II we describe the experimental procedure of data reduction and the determination of the radial-scattering distribution function. In Sec. III we discuss the EXAFS results for bcc Fe and TiFe. In Sec. IV the analysis of the near-edge structure of TiFe is presented. The conclusions of this work are summarized in Sec. V.

II. EXPERIMENTAL

The source of soft x rays was the storage-ring Adone operated at 1.5 GeV and 50 mA. The x rays were monochromatized by a Si(220) channel-cut single crystal at about 17 m from the tangent point. The measured resolution at the Fe K edge was better than 10^{-4} with a second harmonic content of less than 0.3%. Further experimental details have been reported elsewhere.[7]

A typical procedure for data processing is illustrated in Fig. 1 for the absorption spectrum of crystalline iron measured at the K threshold on homogeneous powder samples. The incident (I_0) and the transmitted (I_1) intensities of the light were optimized so that the optical density $\mu d \simeq 2$. The relative modulation of the absorption coefficient

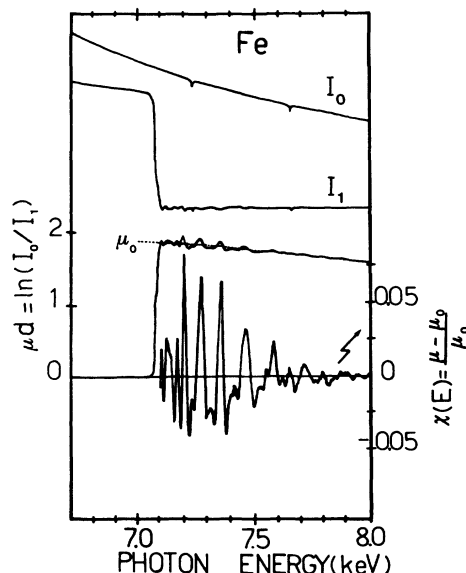$$\chi(k) = \frac{\mu - \mu_0}{\mu_0} , \qquad (1)$$

FIG. 1. EXAFS spectrum at the K edge of bcc Fe. The incident I_0 and transmitted I_1 intensities contain irregularities which are completely compensated in the absorption spectrum.

which is obtained after subtraction of the preedge and of the atomic (μ_0) contributions, was about 10% of the whole absorption at the edge. To avoid uncertainties associated with the best choice of μ_0, we have used the alternative fast Fourier filtering technique to generate $\chi(k)$. This technique consists of eliminating the lowest- and highest-frequency components of the power spectrum, which are related to the background noise and to the edge jump,
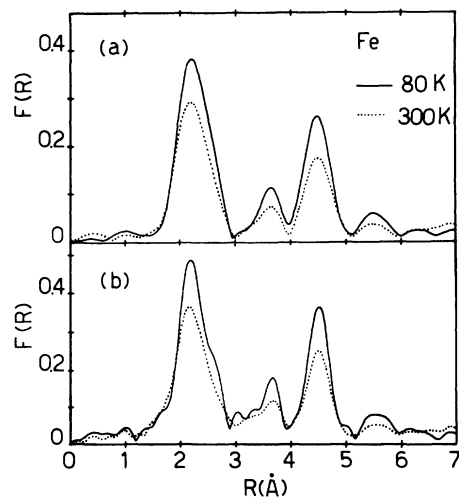

FIG. 2. Radial distribution functions of iron at 80 and 300 K calculated from the data of Fig. 1; (a) with a Gaussian window function and (b) with a Hanning window function.

TABLE I. Parameters used in the model calculation of EXAFS for Fe and TiFe. For the shells of TiFe the reference atom is Fe.

Shell	N	σ_j^2 (10^{-3} Å^2)	R_j (Å)
		Fe	
1	8	2.6	2.482
2	6	3.1	2.866
3	12	4	4.053
4	24	4	4.752
5	8	6	4.971
6	6	8	5.74
S_0^2		0.4	
E_0 (eV)		7112	
		TiFe	
1	8 (Ti)	5	2.579
2	6 (Fe)	5	2.978
3	12 (Fe)	7	4.211
4	24 (Ti)	7	4.938
5	8 (Fe)	8	5.158
6	6 (Fe)	8	5.956
S_0^2		0.4	
E_0 (eV)		7112	

respectively, by limiting the transformation range typically between the harmonic numbers 6 and 50. The $X(k)$ spectra obtained from both methods were identical. The radial distribution functions $F(R)$ at the Fe site are presented in Fig. 2 for $T = 300$ and 80 K. In part (a) we have used a Gaussian window function to multiply $kX(k)$, whereas in part (b) a Hanning function has been employed. As expected, the resolution is better in the latter case, but the spectrum is rich in randomly distributed sidelobes of the main peaks.

III. RESULTS AND DISCUSSION

A. bcc Fe

Because the CsCl structure is similar to that of bcc Fe, it is interesting to regard the $F(R)$ of Fe, shown in Fig. 2, as characteristic of that of TiFe. The modulation function $kX(k)$ and the theoretical radial distribution function of iron, as calculated from the standard single-scattering theory of EX-AFS,[8] are compared in Figs. 3(a) and 3(b) with the corresponding experimental curves. The integration range used ($2.5-15$ Å^{-1}) is the same in both cases. The scattering amplitudes and phases used in the calculation are taken from Teo and Lee's tabulations,[9] and the Debye-Waller factors σ^2 for the first two shells, those estimated by Sevillano et al.,[10] are listed in Table I. The energy scale has been fixed by choosing the reference energy E_0 at the onset of the
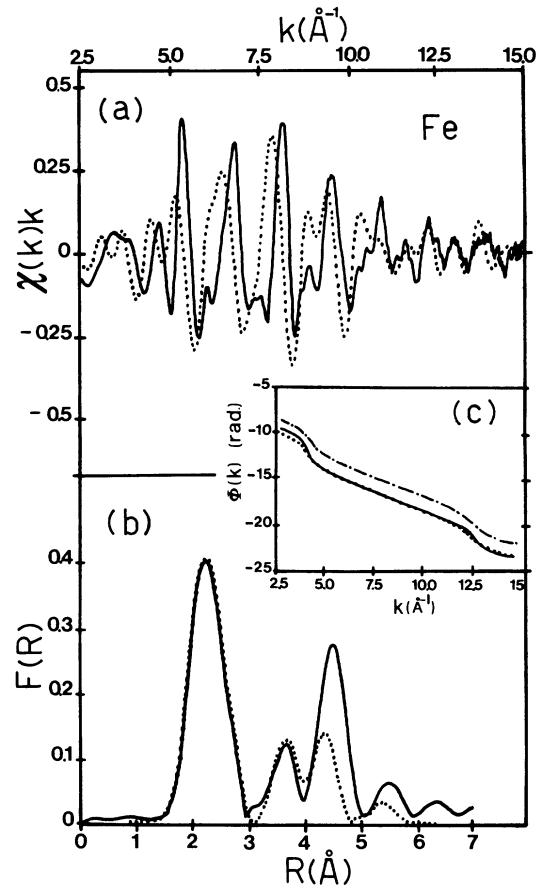
FIG. 3. Comparison between experimental spectra and model calculations: (a) experimental (solid line) and theoretical $kX(k)$ (dotted line) using the raw Teo and Lee phases. (b) Radial distribution functions obtained from the Fourier transform of the above curves. (c) Experimental (solid line) and theoretical (dashed-dotted line) phase shifts obtained from the backtransform of the first peak of the $F(R)$ in (b). The dotted curve is obtained from another calculation with an additional constant shift $\Delta\Phi = -1.6$ rad to the phases of Ref. 9.

Fe K edge at 7112 eV. The theoretical $kX(k)$ curve of Fig. 3(a) has been multiplied by an amplitude reduction factor $S_0^2 = 0.4$, which accounts for many-body and thickness effects.[11] We note that this curve is shifted by a nearly k-independent factor with respect to the experimental one, so that the radial distribution functions of the first shells of Fig. 3(b) are coincident within ± 0.02 Å. Attempts to compensate for this phase difference by changing E_0 result in a mismatch of the peaks' position of the corresponding $F(R)$ transform. Similar discrepancies have been reported in other cases.[12,13] According to Pettifer[14] this could be caused by the use of plane rather than spherical waves in the scattering theory, which is inadequate for heavy atoms and

TABLE II. Corrections $\Delta\Phi$ to the plane-wave phase shifts using the scattering functions $F(\pi,k)$ of Refs. 9 and 16.

E_{kin} (eV)	k (Å^{-1})	Teo and Lee		Fink and Ingram	
		$F(\pi,k)$ (Å)	$\Delta\Phi$ (rad)	$F(\pi,k)$ (Å)	$\Delta\Phi$ (rad)
100	5.13	0.575	−1.37	0.64	−1.69
250	8.11	0.613	−2.46	0.77	−3.87
500	11.47	0.339	−1.06	0.43	−1.70
1000	16.21	0.140	−0.26	0.19	−0.50

small interatomic distances. In the case of ZnSe and ZnTe a nearly constant correction of about −1.5 rad to the Teo and Lee phases is required for the first shell.[14]

The phase difference between plane-wave and spherical-wave calculations is roughly estimated by taking for the effective radius of the backscattering potential the amplitude $F(\pi,k)$. From simple geometrical arguments, $\Delta\Phi$ at the edge of the scattering region is given by[15]

$$\Delta\Phi \cong -2k\frac{[F(\pi,k)]^2}{r_j} , \qquad (2)$$

where r_j is the distance of the jth coordination shell. This correction can be applied to the Teo and Lee phases which are independent of shell radii. We have estimated $\Delta\Phi$ using the backscattering ampli-

tudes of Fe from Teo and Lee and those of Co from Fink and Ingram.[16] The values are listed in Table II. In Fig. 3(c) we report the experimental and theoretical phases for the first two shells of Fe before and after a correction of $\Delta\Phi = -1.6$ rad. Now the agreement with the experimental $F(R)$ and $k\chi(k)$ is rather good, as shown in Fig. 4. From Eq. (2), $\Delta\Phi$ decreases with increasing the shell distance, but this trend is not clearly observed experimentally in Fe. A similar behavior occurs in Ni metal where the $F(R)$ distributions of the inner coordination shells can be analyzed separately. Although the above treatment is certainly rather crude, we believe that it is useful to understand the discrepancy between theoretical and experimental phases usually found for large atomic number elements.

It is clear from Fig. 4(a) that the position, intensity, and spectral width of the more distant shells differ significantly from those of the simulated spec-
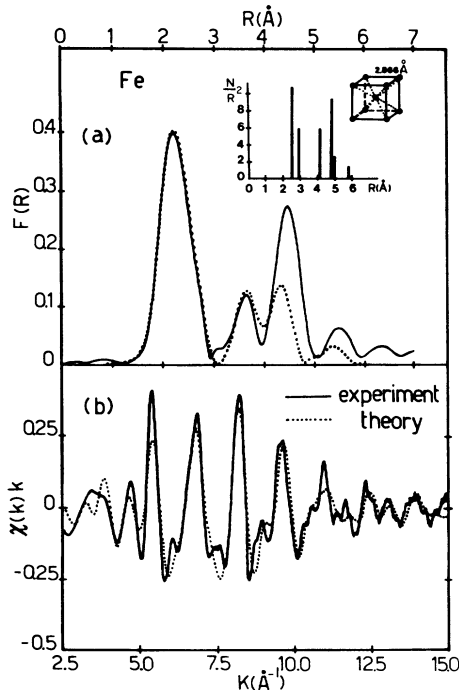

FIG. 4. Comparison between experimental spectra and model calculations of (a) the radial distribution function and (b) the EXAFS of iron.
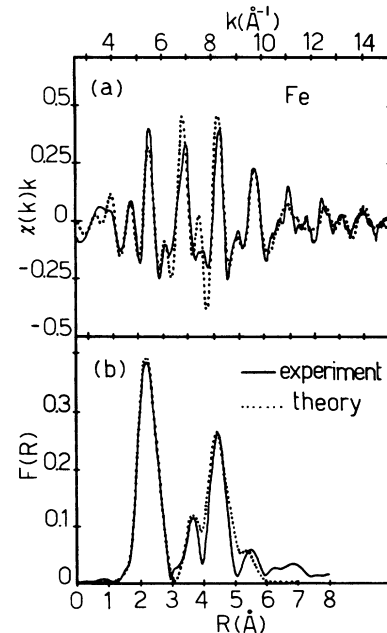

FIG. 5. Same as in Fig. 4 but with the inclusion of multiple scattering for the fifth and sixth coordination shells.

trum; namely, the amplitude of the fourth, fifth, and sixth shells are much stronger in the experimental spectrum. As a consequence, an additional sizeable modification is needed to explain the anomalous intensity of the outer shells due to focusing effects.[15] The single-scattering theory has to be modified to include multiple-scattering processes. For a three-atom system—A and C with the intervening atom B—the contribution from all scattering pathways originating and terminating to the absorbing atom A is[17]

$$k\chi(k) = \frac{F_c(\pi,k)}{r_{ac}^2}\Omega_B(\beta,k)e^{-2\sigma_c^2 k}$$

$$\times \sin[2kr_{ac} + \Phi_{ac}(k) + \omega_B(\beta,k)]$$

$$\times \exp[-2r_{ac}/\lambda(k)] , \quad (3)$$

where $\Omega_B(\beta,k)$ and $\omega_B(\beta,k)$ are the corrected amplitude and phase functions in presence of the scattering atom B. In iron the fifth and sixth coordination shells are shadowed by the first- and second-shell atoms aligned along the cube diagonals and along the perpendicular to the cube faces, respectively. With this atomic disposition a strong enhancement of their amplitude is expected. For forward scattering ($\beta=0$) we can write

$$\Omega_B(0,k) = 1 + \frac{8}{r_{ac}}F_B(0,k)\cos\theta_B(0,k)$$

$$+ \left[\frac{4}{r_{ac}}F_B(0,k)\right]^2 , \quad (4)$$

$$\omega_B(0,k) = 2\tan^{-1}\left[\frac{(4/r_{ac})F_B(0,k)\sin\theta_B(0,k)}{1+(4/r_{ac})F_B(0,k)\cos\theta_B(0,k)}\right] ,$$

$$(5)$$

where $r_{ac} = 2r_{ab}$ are the interatomic distances of the 5th and 6th shells, and $F_B(0,k)$ and $\theta_B(0,k)$ are the forward amplitude and phase functions of the atom B, respectively. These functions have been tabulated by Fink and Ingram[16] for the scattering of low-energy electrons (kinetic energies less than 1500 eV) on free atoms. Using these functions, we have computed $k\chi(k)$ from Eq. (3) and its Fourier transform. They are displayed in Fig. 5. It is apparent that the fifth and sixth shells are now in better agreement with the experiment than they are in Fig. 4 as regards their position, width, and relative intensity. The atomic data, however, overestimate the experimental intensity and must be scaled down by a constant factor. Weak sensitivity to k of the multiple-scattering terms has been reported for Cu, where the amplitude function $F(0,k)$ of Fink and Ingram at a

single k value is sufficient to explain the enhancement of the fourth coordination shell, but $\theta_B(0,k)$ is in disagreement with the experimental data.[18] The inclusion of all multiple-scattering paths involving the fourth shell, which consists of 24 atoms located at 4.752 Å, would add to $\chi(k)$ an additional term with $\beta=\pi/4$ rad, i.e.,

$$\Omega_B = \{4A^2(2\sin\gamma + A\sin2\gamma)^2$$

$$+ [1+2A(2\cos\gamma + A\cos2\gamma)]^2\}^{1/2} , \quad (6)$$

$$\omega_B = \tan^{-1}\left|\frac{2A(2\sin\gamma + A\sin2\gamma)}{1+2A(2\cos\gamma + A\cos2\gamma)}\right| , \quad (7)$$

with

$$A = \frac{r_{ac}}{r_{ab}r_{bc}}F_B(\beta,k)$$

$$\times \exp[-(r_{ab}+r_{bc}-r_{ac})/\lambda] , \quad (8)$$

$$\gamma = \theta_B(\beta,k) + k(r_{ab}+r_{bc}-r_{ac}) . \quad (9)$$

Since $F_B(\pi/4,k)$ is between 5 and 10 times smaller than $F_B(0,k)$ at low k and attenuates rapidly at high k,[16] this additional corrective term will produce only minor changes to $F(R)$ and we therefore conclude that its contribution to $\chi(k)$ is negligible. So, even if an unequivocal determination of the forward scattering amplitude and phases is not possible with the present data, we clearly recognize that the consideration of multiple-scattering effects is essential to explain the $F(R)$ distribution of the outer shells of bcc iron.

The first-nearest-neighbor shells at 2.485 and 2.866 Å cannot be directly resolved because the highest resolution attainable for a simple sine-wave
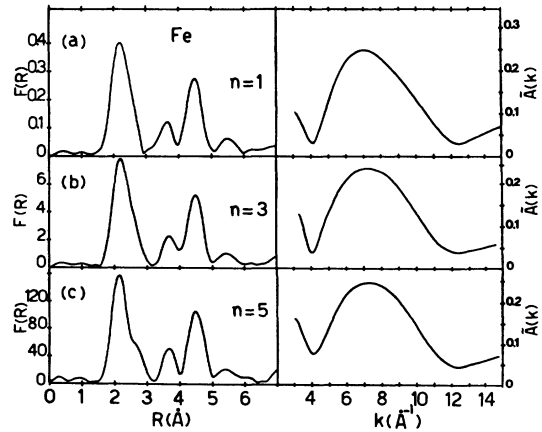

FIG. 6. Radial distribution function and amplitude of the first peak of $F(R)$ for Fe calculated for three values of n and for a Gaussian window function.
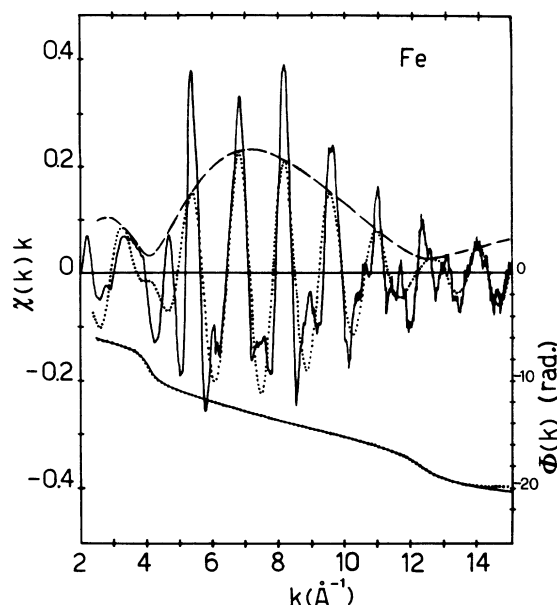
FIG. 7. Back-Fourier transform $k\chi(k)$ of the first peak of the experimental radial distribution function of Fe (dotted line), its envelope function $\tilde{A}(k)$ (dashed line), and phase functions at 80 and 300 K. For comparison the total experimental spectrum of $k\chi(k)$ is shown.

function Fourier transform is $\Delta r = 2\pi/(k_{max} - k_{min}) = 0.5$ Å for a transformation range $\Delta k = 12$ Å. In practice, the resolution is further reduced by the window function which is introduced to eliminate truncation effects associated with the finite integration range of the Fourier transform. The
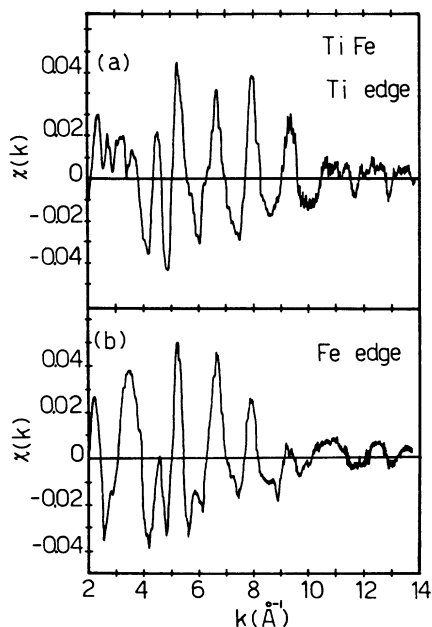

FIG. 8. EXAFS modulation of TiFe above the (a) Ti and (b) Fe edges.

Gaussian window yields generally lower resolution than the Hanning-type window but has the effect of considerably reducing the amplitude of the sidelobes. Apparently, the first peak of $F(R)$ can be split into its two components by using the Hanning function, and multiplying $\chi(k)$ by k^n to compensate for the k dependence of the backscattering amplitudes at large k values.[19] However, we have found that this result is greatly dependent upon the value of n and/or on the apodization value used for the window function. Moreover, the peak positions move appreciably with n. We have verified that the phase linearization procedure of Ref. 19, requiring a shift of E_0 of -32 eV, makes the positions of the first and third peaks largely independent of n, but removes any structure associated with the second peak. In addition, a discrepancy is observed in the fourth peak which, according to our previous discussion, is made of two shells and is strongly affected by multiple scattering. However, using a Gaussian window, we have found that the first peak of $F(R)$ is essentially insensitive to the value of n used in the Fourier transform (within ± 0.02 Å), in distinction to the behavior observed in Ni where a Hanning function is used.[19] This can be seen in Fig. 6, which displays the radial distribution $F(R)$ calculated with three different weighting factors and the corresponding back-Fourier amplitude of the first peak. We believe that conclusive evidence of the first peak splitting is hardly attainable from direct inspection of the Fourier-transform spectra. Therefore, the alternative approach which we have adopted is the beat method.[20] By backtransforming the first peak of $F(R)$ in Fig. 4 between 1.2 and 3.0 Å we obtain the $k\chi(k)$ for this shell shown in Fig. 7. The minima of the envelope function correspond to inflection points of the phase and the separation ΔR of the component shells, reported in Table III, agrees well with the calculated values from the known lattice parameter. It is interesting to note
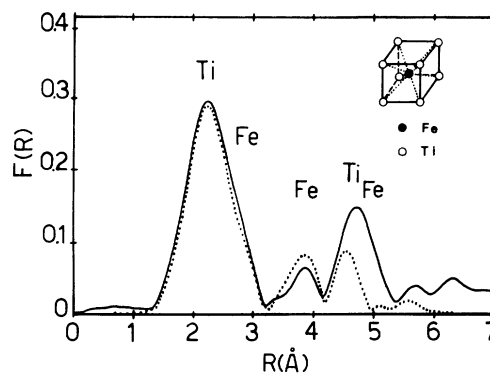

FIG. 9. Radial distribution function of TiFe around the iron atom. The dotted curve is a single-scattering model calculation.
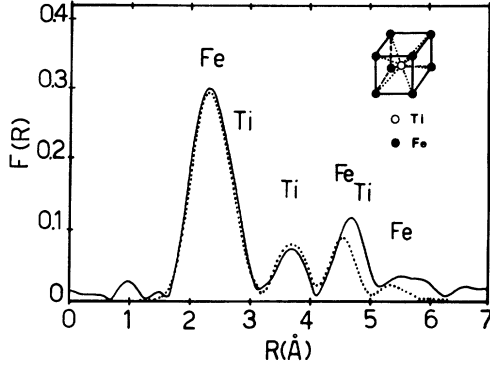
FIG. 10. Radial distribution function of TiFe around the titanium atom. The dotted curve is a single-scattering model calculation for the first two shells.

that the experimental phases for two different temperatures are coincident over an extended k range, indicating that the difference in the mean-square relative displacement of the first two shells at 80 and 300 K is small, in accordance with the theoretical estimates.[10] Moreover, effects of anharmonicity of the scattering potential[21] are negligible.

B. TiFe

The EXAFS oscillations $\chi(k)$ above the K edges of Ti and Fe are shown in Fig. 8 for TiFe. The corresponding radial distribution functions around the Fe and Ti atoms, displayed in Figs. 9 and 10, resemble those of pure Fe except for the different relative intensities of the peaks which correspond to iron and titanium coordination shells. The first peak of $F(R)$ at the Fe edge occurs at 2.25±0.03 Å, close to its theoretical position 2.22±0.03 Å. Its line shape can be accurately reproduced by a model calculation of $F(R)$ which incorporate six shells[22] and uses a Debye-Waller term compatible with the Debye temperature of TiFe, $\Theta_D = 450$ K (see Table I). The
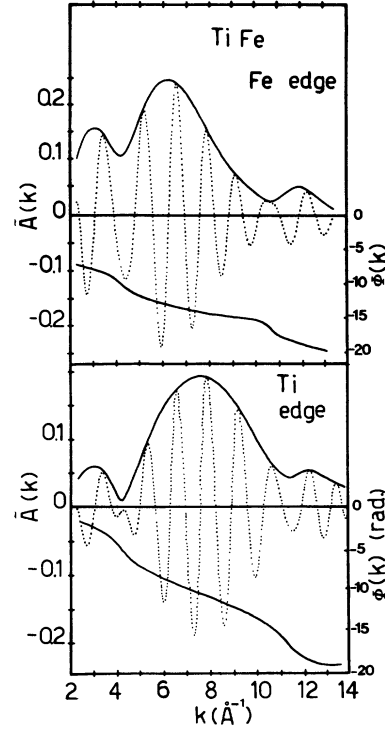

FIG. 11. Back-Fourier transform of the first peak of the experimental $F(R)$ of TiFe. $k\chi(k)$ (dotted line), $\tilde{A}(k)$ envelope function, and $\Phi(k)$ phase function around the Ti and Fe edges.

neighboring Ti and Fe shells beat at values of k for which[7]

$$\Delta R = \frac{n\pi - \Delta\Phi_{TiFe}}{2k_{min}} \quad (n = 1,3,\dots) \quad (10)$$

where $\Delta\Phi_{TiFe}$ is the phase difference between the backscattering phases of Ti and Fe evaluated at the beating minima (Fig. 11). The estimation of ΔR from Eq. 10, making use of the Teo and Lee phases, is given in Table III. We remark that the phase

TABLE III. Comparison of differences in bond lengths of the first two coordination shells of Fe and TiFe determined with the beat method ΔR_{beat} and calculated from known lattice constants ΔR_{cal}.

Edge	n	k_{min} (Å^{-1})	ΔR_{beat} (Å)	ΔR_{cal} (Å)
		Fe		
Fe	1	4.12	0.381	0.381
	3	12.40	0.380	
		TiFe		
Ti	1	4.20	0.367	0.399
	3	11.50	0.440	
Fe	1	4.22	0.396	0.399
	3	10.78	0.406	

FIG. 12. (a) XANES of the Ti K edge of TiFe and its energy derivative spectrum (dotted line); (b) same for Ti metal.
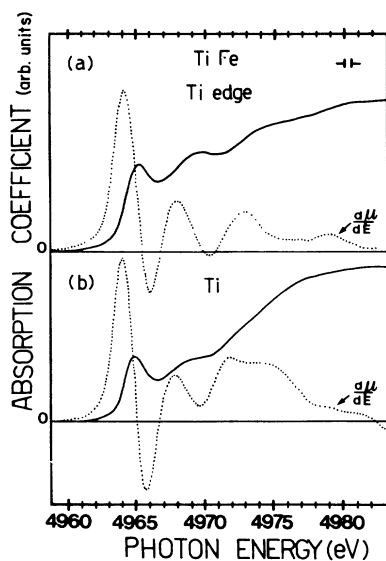

FIG. 13. (a) XANES of the Fe K edge of TiFe and its energy derivative spectrum (dotted line); (b) same for Fe metal.

correction $\Delta\Phi$ of Eq. 2 is nearly the same for both Fe and Ti,[7] and thus cancels in Eq. (10). The resulting shell separation agrees with diffraction data. The intensity of the fifth and sixth shells in Figs. 9 and 10 is smaller when the intermediate first-shell atom is Fe, because its forward scattering power is lower than that of Ti. On the other hand, the importance of multiple-scattering corrections on the outer shells is evident from Figs. 9 and 10 where the single-scattering model calculation of $F(R)$ is compared with the experiment. Owing to the uncertainties connected with the forward scattering amplitude and phase for the Ti-Fe pair, we did not attempt an explicit calculation of the multiple-scattering contribution in TiFe.

The radial distribution function around Ti of Fig. 10 looks like the function around Fe with minor modifications. The nearest-neighbor peak occurs experimentally at 2.31 ± 0.03 Å and is significantly narrower than the function around Fe. As the model calculation shows (dotted line), this is associated with the weaker backscattering strength of the Ti shell at 2.978 Å. The beating analysis applied to the first peak of $F(R)$ gives the scattering amplitude $\widetilde{A}(k)$ shown in Fig. 11 around Ti with two distinct minima at $k=4.20$ and $k=11.5$ Å^{-1}. Equation (10) then provides the shell separation listed in Table III. We stress that the peak position of $F(R)$ around different absorbers, their line shape, and the beating minima of $\widetilde{A}(k)$ indicate that the sequence of the scattering shells is definitely the same as that of the CsCl structure, a result which cannot be directly obtained from x-ray diffraction.[3]
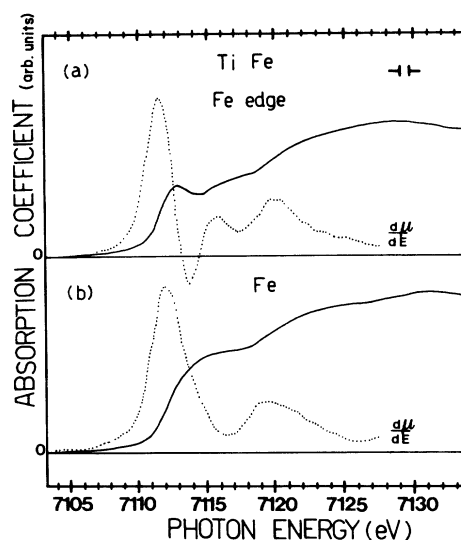
IV. XANES OF TiFe

The K-edge absorptions of Ti (4964 eV) and Fe (7112 eV) in TiFe are displayed in Figs. 12 and 13, respectively. The spectral line shapes are both similar to those of Ti metal, shown in the lower panel of Fig. 12, and reflect the p component of the partial density of states of the conduction band of Ti near the K edge. The spectral distribution of iron, shown in Fig. 13(b), is actually strongly different from that of titanium. The dominant contribution of titanium to the lowest conduction-band states of TiFe is predicted by accurate partial—density-of-states calculations. To stress this point we report in Fig. 14 the spectral shape at the Ti and Fe edges of the partial p-like and d-like densities of states computed by Papaconstantopoulos.[5] To facilitate the comparison with the experiment, we have convoluted the theoretical histograms with a Lorentzian distribution function with a full width at half maximum of 1.3 and 1.5 eV for Ti and Fe, respectively, which accounts for the Auger lifetime of the $1s$ hole[23] and for the spectrometer resolution. Once more it is apparent that only the projected density of states of p-like symmetry at the excited atom site describes rather accurately the near K-edge line shape, at least within 10 eV from the edge. The relative intensities of the structures depend also on the transition probability. Since the radial matrix element is a smooth function of the energy, its inclusion will not introduce extra peaks and the XANES will reflect mainly the density-of-states curve of the appropriate symmetry and site.[7] The partial density of states calculated from the band structure should be equivalent
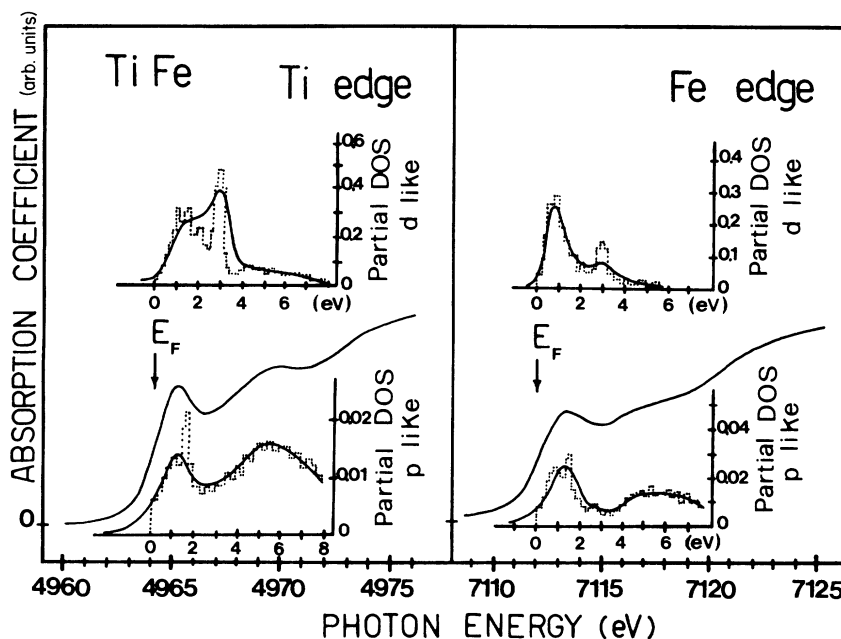
FIG. 14. Partial d- and p-like densities of the conduction-band states of TiFe at the Ti and Fe sites, compared with the experimental XANES.

to that obtained from multiple-scattering calcula-
tions, provided the same atomic muffin-tin potential
is used in both models.

The position of the Fermi energy E_F, as deter-
mined by the peak of the first energy derivative
spectrum, coincides at the Ti edge in the metal and
in the alloy, in agreement with the results of the Ti
K emission.[24] At the Fe K edge, E_F is slightly shift-
ed towards a lower energy of about 0.3 eV relative to
the pure metal edge. Since the energy shifts of the
inner levels $1s$, $2p$, and $3p$ of iron are negligible,[24,25]
this displacement is ascribed to a higher occupancy
of the conduction states of the metal with respect to
the alloy. Similar results have been found in other
Asano alloys.[24]

V. CONCLUSIONS

We have shown that a detailed analysis of the
EXAFS spectrum of bcc iron provides the basic

structural information needed to understand the
atomic environment of the intermetallic CsCl lattice
of TiFe around Ti and Fe atoms. Multiple-
scattering effects typical of the bcc structure are sin-
gled out for the fifth and sixth shells of the metal
and of the alloy. The plane-wave approximation for
the scattering is found to be inadequate and a
correction factor independent of k has to be applied
to the backscattering phase shifts to bring theoreti-
cal and experimental $k\chi(k)$ into agreement. With
this correction to the phase the reference energy E_0
is placed at the edge onset, while without any
correction, E_0 has to be shifted by a large amount
($+10-15$ eV) in order to fit the experimental
$k\chi(k)$. The XANES of Ti and Fe K edges directly
probe the local state density of p-like symmetry for
the conduction band of TiFe. The empty p-like den-
sities of states are very similar in shape for both
sites to that of titanium, in accordance with previ-
ous theoretical estimates.

[1]See, e.g., Proceedings of the International Symposium on
the Properties and Applications of Metal Hydrides,
Colorado Springs, 1980 [J. Less-Common Met. 73, 1
(1980)].

[2]D. H. Polonis and J. G. Parr, Trans. Metall. Soc. AIME
200, 1148 (1954).

[3]T. V. Philip and P. A. Beck, Trans. Metall. Soc. AIME
209, 1269 (1957).

[4]J. Yamashita and S. Asano, Prog. Theor. Phys. 48, 2119
(1972).

[5]D. A. Papaconstantopoulos, Phys. Rev. Lett. 31, 1050
(1973).

[6]D. A. Papaconstantopoulos, Phys. Rev. B 11, 4801
(1975).

[7]A. Balzarotti, M. De Crescenzi, and L. Incoccia, Phys.
Rev. B 25, 6349 (1982).

[8]D. E. Sayers, E. A. Stern, and F. W. Lytle, Phys. Rev. Lett. 32, 1204 (1971); E. A. Stern, Phys. Rev. B 10, 3027 (1974).

[9]B. K. Teo and P. A. Lee, J. Am. Chem. Soc. 101, 2815 (1979).

[10]E. Sevillano, H. Meuth, and J. J. Rehr, Phys. Rev. B 20, 4908 (1979).

[11]P. A. Lee, P. H. Citrin, P. Eisenberger, and B. M. Kincaid, Rev. Mod. Phys. 53, 769 (1981).

[12]M. De Crescenzi, A. Balzarotti, F. Comin, L. Incoccia, S. Mobilio, and N. Motta, Solid State Commun. 37, 921 (1981).

[13]R. F. Pettifer and P. W. McMillan, Philos. Mag. 35, 871 (1977).

[14]R. F. Pettifer, in Inner-Shell and X-Ray Physics of Atoms and Solids, edited by D. J. Fabian, H. Kleinpoppen, and L. M. Watson (Plenum, New York, 1980).

[15]P. A. Lee and J. B. Pendry, Phys. Rev. B 11, 2795 (1975).

[16]M. Fink and J. Ingram, At. Data 4, 129 (1972).

[17]B. K. Teo, J. Am. Chem. Soc. 103, 3990 (1981).

[18]P. Rabe, in Proceedings of the Daresbury Study Weekend, compiled by C. D. Garner and S. S. Hasnain, Daresbury Lab Report No. DL/SCI R17,76 (unpublished).

[19]M. B. Stearns, Phys. Rev. B 25, 2382 (1982).

[20]G. Martens, P. Rabe, N. Schwentner, and A. Werner, Phys. Rev. Lett. 39, 1411 (1977).

[21]P. Eisenberger and G. S. Brown, Solid State Commun. 29, 481 (1979).

[22]E. A. Starke, C. H. Cheng, and P. A. Beck, Phys. Rev. 126, 1746 (1962).

[23]V. O. Kostroun, M. H. Chen, and B. Crasemann, Phys. Rev. A 3, 533 (1971).

[24]E. Kallne, J. Phys. F 4, 167 (1974).

[25]J. H. Weaver and D. T. Peterson, Phys. Rev. B 22, 3624 (1980).